0026-895X/02/6203-529–538$7.00
MOLECULAR PHARMACOLOGY
Vol. 62, No. 3
1559/1008151
Mol Pharmacol 62:529–538, 2002
Printed in U.S.A.

Arsenic Trioxide Produces Polymerization of Microtubules and Mitotic Arrest before Apoptosis in Human Tumor Cell Lines

YI-HE LING, JIAN-DONG JIANG, JAMES F. HOLLAND, and ROMAN PEREZ-SOLER

Departments of Medicine (Y.-H.L.) and Oncology (R.P.-S.), Albert Einstein College of Medicine, Bronx, New York; Department of Medicine, Mount Sinai School of Medicine, New York, New York (J.-D.J., J.F.H.); and Institute of Medicinal Biotechnology, Chinese Academy of Medical Sciences and Peking Union Medical College, Beijing, People's Republic of China (J.-D.J)

Received December 19, 2001; accepted June 10, 2002

This article is available online at http://molpharm.aspetjournals.org

ABSTRACT

Arsenic trioxide (As_2O_3) has been found to induce apoptosis in leukemia cell lines and clinical remissions in patients with acute promyelocytic leukemia. In this study, we investigated the cytotoxic effect and mechanisms of action of As_2O_3 in human tumor cell lines. As_2O_3 caused inhibition of cell growth (IC_{50} range, 3–14 μM) in a variety of human solid tumor cell lines, including four human non–small-cell lung cancer cell lines (H460, H322, H520, H661), two ovarian cancer cell lines (SK-OV-03, A2780), cervical cancer HeLa, and breast carcinoma MCF-7, as assessed by 3-(4,5-dimethylthiazol-2-yl)-2,5-diphenyltetrazolium bromide assay. Flow cytometry analysis showed that As_2O_3 treatment resulted in a time-dependent accumulation of cells in the G_2/M phase. We observed, using Wright-Giemsa and 4′,6-diamidine-2-phenylindole-dihydrochloride staining, that As_2O_3 blocked the cell cycle in mitosis. In vitro examination revealed that As_2O_3 markedly promoted tubulin polymerization without affecting GTP binding to β-tubulin. Immunocytochemical and EM studies of treated MCF-7 cells showed that As_2O_3 treatment caused changes in the cellular microtubule network and formation of polymerized microtubules. Similar to most anti-tubulin agents, As_2O_3 treatment induced up-regulation of the cyclin B1 levels and activation of $p34^{cdc2}$/cyclinB1 kinase, as well as Bcl-2 phosphorylation. Furthermore, activation of caspase-3 and -7 and cleavage of poly-(ADP-ribose) polymerase and β-catenin occurred only in As_2O_3-induced mitotic cells, not in interphase cells, suggesting that As_2O_3-induced mitotic arrest may be a requirement for the activation of apoptotic pathways. In addition, As_2O_3 exhibited similar inhibitory effects against parental MCF-7, P-glycoprotein–overexpressing MCF-7/doxorubicin cells, and multidrug resistance protein (MRP)-expressing MCF-7/etoposide cells (resistance indices, 2.3 and 1.9, respectively). Similarly, As_2O_3 had similar inhibitory effect against parental ovarian carcinoma A2780 cells and tubulin mutation paclitaxel-resistant cell lines PTx10 and PTx22 (resistance indices, 0.86 and 0.93, respectively), suggesting that its effect on tubulin polymerization and G_2/M phase arrest is distinct from that of paclitaxel. Taken together, our data demonstrate that As_2O_3 has a paclitaxel-like effect, markedly promotes tubulin polymerization, arrests cell cycle at mitosis, and induces apoptosis. In addition, As_2O_3 is a poor substrate for transport by P-glycoprotein and MRP, and non–cross-resistant with paclitaxel resistant cell lines due to tubulin mutation, suggesting that As_2O_3 may be useful for treatment of human solid tumors, particularly in patients with paclitaxel resistance.

Recent evidence has indicated that arsenic trioxide (As_2O_3) is able to induce clinical remissions in patients with acute promyelocytic leukemia (APL) (Chen et al., 1997; Look, 1998; Shao et al., 1998; Soignet et al., 1998). In addition, several investigators have shown that As_2O_3 induces programmed cell death in APL cell lines with APL/RA proteins. Although the mechanisms by which As_2O_3 induces apoptosis remain to be further elucidated, some evidence indicated that this compound can down-regulate Bcl-2 protein and activate caspase-3–like caspase activity (Chen et al., 1996, 1998; Kroemer and de The, 1999). Some investigators have shown that As_2O_3-induced apoptosis is caused by a direct effect on the mitochondrial permeability transition pore and loss of the mitochondrial transmembrane potential (Zhu et al., 1999).

Microtubules are critical elements in a wide variety of fundamental functions, including sustained cell shape, cellular transportation of vesicles and protein complexes, and regulation of cell motility, as well as of cell division (Hyams and Lloyd, 1993; Margolis and Wilson, 1998). During mitosis, microtubules are at the highest dynamic instability for re-

This work was supported in part by National Institutes of Health grant CA50270 and by the T. J. Martell Foundation for Leukemia, Cancer, and AIDS Research.

Y.-H. L. and J.-D. J. made equal contributions to this work.

ABBREVIATIONS: APL, acute promyelocytic leukemia; NSCLC, non–small-cell lung cancer; Dox, doxorubicin; VP-16, etoposide; PARP, poly(ADP-ribose) polymerase; DAPI, 4′,6-diamidine-2-phenylindole-dihydrochloride; PBS, phosphate-buffered saline; MES, 2-(*N*-morpholino)ethanesulfonic acid; DTT, 1,4-dithiothreitol; CHAPS, 3-[(cholamidopropyl) dimethylammonio]-1-propane-sulfonate; pNA, *p*-nitroanilide; Ac, *N*-acetyl; RI, resistance index; PD98059, 2′-amino-3′-methoxyflavone; MDR, multidrug resistance; MRP, multidrug resistance protein.

sponse to the formation of spindles and separation of chromosomes. Because microtubules play crucial roles in the regulation of the mitotic apparatus, disruption of microtubules can induce cell-cycle arrest in M-phase, formation of abnormal mitotic spindles, and final triggering of the signals for programmed cell death (Mitchison, 1988). Agents such as the vinca alkaloids and the taxanes, which affect the dynamics of microtubules, have emerged as useful therapeutic agents for the treatment of human cancer (Rowinsky and Donehower, 1991; Jordan et al., 1992). Recently, some reports indicated that As_2O_3 treatment resulted in cell-cycle arrest at either G_1 or G_2/M phase depending on the cell lines (Ma et al., 1998; Perkins et al., 2000). In addition, Li and Broome reported that As_2O_3 treatment resulted in cell-cycle progression arrest at metaphase in myeloid leukemia cells through noncompetitive disruption of GTP binding to β-tubulin and inhibition of GTP-induced tubulin polymerization (Li and Broome, 1999).

Although a number of studies have demonstrated that As_2O_3 has potent activity against cell growth in a series of leukemia cell lines, little information is available regarding this compound's effect on cell growth in solid tumor cell lines (Seol et al., 1999; Meada et al., 2001). In this study, we investigated the effect of As_2O_3 on cell proliferation in human solid tumor cell lines, particularly breast, ovary, and lung. Moreover, we also investigated the molecular basis of As_2O_3-induced cell cycle arrest and apoptosis in human breast carcinoma MCF-7 cells and NSCLC H460 cells. Interestingly, we found that As_2O_3 treatment led to the accumulation of cells in mitosis, and the induction of apoptosis. Further studies showed that As_2O_3 caused a paclitaxel-like concentration-dependent promotion of tubulin polymerization in vitro. Morphological and EM observations showed that As_2O_3 caused changes in the cellular microtubule network.

Because As_2O_3 had a paclitaxel-like effect, it was of great interest to test whether As_2O_3 could circumvent paclitaxel resistance. The results present herein show that As_2O_3 is active in paclitaxel resistant cell lines, whether due to overexpression of P-glycoprotein, or MRP, or tubulin mutation.

Overall, our results lead to a better understanding of the unique mechanism of action of As_2O_3, and provide a suggestion that As_2O_3 may be of therapeutic value for the treatment of human solid tumors including those with acquired resistance.

Materials and Methods

Cell Culture and Treatment. Human cervical HeLa cells, ovarian cancer SK-OV-03 cells, and human NSCLC cell lines, H460, H322, H520, and H661 were purchased from the American Type Culture Collection (Manassas, VA) and maintained in RPMI 1640 medium supplied with 10% fetal bovine serum. Human breast carcinoma MCF-7 cells, P-glycoprotein–overexpressing MCF-7/Dox cells, and MRP-positive MCF-7/VP-16 cells were maintained in culture as monolayers in minimal essential medium with 10% fetal bovine serum as described previously (Perez-Soler et al., 1997). Human ovarian carcinoma A2780 cells and the tubulin mutant cell lines resistant to paclitaxel (A2780/PTx10, A2780/PTx22) were kindly provided by Dr. Fojo (National Cancer Institute, National Institutes of Health, Bethesda, MD). A2780 cells were maintained in RPMI 1640 medium with 10% fetal bovine serum, A2780/PTx10 and A2780/PTx22 cells were maintained in the same medium containing 15 ng/ml of paclitaxel and 5 μg/ml of verapamil (Giannakakou et al., 1997). For determination of cell growth inhibition, cells were plated at 1×10^4 cells/well in 96-well microplates and exposed to varying concentrations of As_2O_3 and paclitaxel at 37°C for 72 h. At the end of drug exposure, 10 μl of 3-(4,5-dimethylthiazol-2-yl)-2,5-diphenyltetrazolium bromide solution (5 mg/ml) was directly added to each cell culture well and the plates were incubated at 37°C for 2 h. The formazan converted from tetrazolium salt by viable cells was solubilized by 100 μl of lysis solution containing 20% SDS and 50% dimethyl formamide (Sigma-Aldrich, St. Louis, MO), and measured in a microplate reader (Dynex Technologies, Chantilly, VA) at 570 nm as described by Hansen et al. (1989). The IC_{50} value resulting from 50% inhibition of cell growth was calculated graphically as a comparison with the control.

Reagents. As_2O_3 was purchased from Sigma Chemical Inc. (St. Louis, MO), and dissolved in 10% NaOH as 20 mM stock solution. Paclitaxel was purchased from Hande Tech Development USA, Inc. (Houston, TX) and dissolved in dimethyl sulfoxide as 1 mM stock solution. Monoclonal anti–cdc-2, anti-cyclin B1, and anti–Bcl-2 antibodies were purchased from Oncogene Science (Cambridge, MA). Anti–β-tubulin antibody was obtained from Biogenex Co. (San Ramon, CA). Anti-PARP and anti–β-catenin antibodies were purchased from BD PharMingen (San Diego, CA). All other chemicals were purchased from Sigma-Aldrich.

Apoptosis Assay. Cells were treated with As_2O_3 for the indicated time. The attached and detached cells were harvested from culture, and stained with DAPI. The cells with nuclear breakage were manually counted by fluorescence microscopy. For assay of DNA fragmentation, cells were treated with As_2O_3 for the indicated time. After treatment, cells were harvested from culture and lysed with lysis buffer containing 0.5% Triton X-100, 100 mM Tris-HCl, pH 7.5, and 25 mM EDTA at 4°C for 60 min. After centrifugation at 15,000*g* for 10 min, the supernatants were collected and treated with 100 μg/ml of RNase I and 100 μg/ml of proteinase K at 50°C for 30 min, and with phenol and chloroform. The fragmented DNA was precipitated in the presence of sodium acetate and ethanol, dissolved in Tris/EDTA buffer, and then subjected to 1% agarose gel. After electrophoresis, DNA was stained with ethidium bromide and visualized by UV light illumination.

Cell Cycle Analysis. Cells were washed with PBS and fixed with cold 75% ethanol overnight. The fixed cells were incubated with 5 μg/ml of RNase I and 1 μg/ml of propidium iodide for 6 h, and then cellular DNA content was determined in a flow cytometer. For quantitative assay of mitotic cells, after staining with Wright-Giemsa dye, at least 100 mitotic cells and those with chromosome condensation were counted.

Tubulin Assembly. Purified tubulin from calf brain was purchased from Sigma-Aldrich. The effects of As_2O_3 on the microtubule assembly-disassembly process were determined as described previously (Jiang et al., 1998b). For assembly assay, 100 μl of tubulin solution (500–600 μg of protein/ml) was mixed gently with 400 μl of reaction buffer containing 0.1 M MES, 1 mM EGTA, 0.5 mM $MgCl_2$, 0.1 mM EDTA, and 2.5 M glycerol at 37°C. As_2O_3 (0.5–2 mM) was added to each sample cuvet, together or 30 min before 1 mM GTP. Microtubule assembly was monitored by measuring the change of absorbance at room temperature at 350 nm every 5 min on a spectrophotometer (Ultrospec III; Pharmacia LKB, Uppsala, Sweden) until the assembly was completed. For disassembly assay, As_2O_3 or paclitaxel were added to a cuvet with polymerized microtubules according to the method as described above, and incubated in ice. Changes in absorbance were monitored at 350 nm for 30 min. An equal amount of solvent was used in control cuvet.

Immunoblot Analysis. Cells were harvested from culture, washed with PBS solution and lysed with buffer containing 50 mM Tris-HCl, pH 7.4, 100 mM NaCl, 1 mM EDTA, 1 mM EGTA, 1 mM DTT, 1 mM phenylmethylsulfonyl fluoride, 0.1% nonylphenoxy polythoxy ethanol, 1% SDS, 5 μg/ml of aprotinin, and 5 μg/ml of leupeptin. The protein amount in each sample was determined with a Bio-Rad DC protein assay kit (Bio-Rad, Hercules, CA). Equal

amounts of lysate were loaded on a 12.5% SDS-polyacrylamide gel. After electrophoresis, proteins were transferred to a nitrocellulose membrane and probed by corresponding antibodies. The protein signals were detected by the enhanced chemiluminescence reaction system according to the manufacturer's recommendation (Amersham Biosciences, Indianapolis, IN). The quantification of protein levels in each sample was performed by laser scanner densitometer (GS-670 scanning densitometer; Bio-Rad).

Histone H1 Kinase Assay. After treatment with As_2O_3, cells were harvested, washed with PBS solution, and lysed with buffer as described above except for the addition of 1% SDS. Lysate was centrifuged at 15,000*g* for 10 min, and the supernatant was harvested for immunoprecipitation. Cdc2/cyclin B1 complex was immunoprecipitated by monoclonal anti-cdc2 and cyclin B1 antibodies at 0 to 4°C overnight, and cdc2/cyclin B1 kinase activity was measured by [γ-^{32}P]ATP incorporation into the substrate histone H1 as described previously (Ling et al., 1996).

Caspase Activity Assay. Cells (2×10^6) were lysed with 50 μl of lysis buffer containing 50 mM HEPES, pH 7.4, 0.1% CHAPS, 1 mM DTT, and 0.1 mM EDTA at 0 to 4°C for 5 min. After centrifugation at 15,000*g* for 15 min, the supernatant was harvested and added to 100 μl of reaction mixture containing 50 mM HEPES, pH 7.4, 100 mM NaCl, 0.1% CHAPS, 10 mM DTT, 1 mM EDTA, 10% glycerol, and 2 mM caspase substrates, which were Ac-Asp-Glu-Val-Asp-pNA for caspase-3, Ac-Tyr-Val-Ala-Asp-pNA for caspase-1, Ac-Ile-Glu-Thr-Asp-pNA for caspase-8, and Ac-Leu-Glu-His-Asp-pNA for caspase-9. After incubation at 37°C for 120 min, caspase activity was assessed by measurement at 405 nm of pNA release from the substrate.

Immunocytochemical Study. Cells were fixed with cold methanol at −20°C for 5 min, and washed with PBS solution. Cells were blocked with 1% bovine serum albumin PBS solution for 30 min, and incubated with monoclonal anti–β-tubulin antibody (1:100) at room temperature for 90 min. After washing three times with PBS solution, cells were reincubated with fluorescein isothiocyanate-conjugated second antibody (1:500) in the dark room for 30 min. Cellular microtubules were observed with a Nikon PS200 fluorescence microscope.

Electron Microscopy. MCF-7 cells were treated with 3 μM As_2O_3 or with the same volume of PBS solution as control. After 12 h, cells were collected and washed twice with PBS solution. Cells were then fixed with osmium tetroxide, dehydrated with an ascending series of ethanol and propylene oxide, and embedded in Araldite. Thin sections were collected on Quick-Coat (Electron Microscopy Sciences, Fort Washington, PA), and treated with copper grids. After staining with uranyl acetate and lead citrate, samples were viewed at 80 kV on a JEOL 1200 EX electron microscope.

Results

Effect of As_2O_3 on Growth and Apoptosis in Human Solid Tumor Cells. The initial experiments were conducted for evaluation of As_2O_3-induced anti-proliferation in various human sold tumor cell lines. Human ovarian cancer A2780 and breast carcinoma MCF-7 cells exhibited the highest susceptibility to As_2O_3, with an IC_{50} ~3.0 μM. Cell lines of cervical (HeLa) and ovarian carcinoma (SK-OV-03) were slightly less sensitive (IC_{50}, 4.28 to 4.61 μM). NSCLC H520, H322, and H460 cells displayed the lowest susceptibility (IC_{50}, >10 μM) (Table 1). Next, we examined whether the inhibition of cell growth by As_2O_3 could be caused by apoptotic death. MCF-7 cells were treated with 3 μM As_2O_3 for the times indicated in Fig. 6. As_2O_3-induced apoptosis was determined both by DAPI staining of cells with nuclear breakage and by DNA fragmentation. As shown in Fig. 1A, only ~2 to 5% of cells were apoptotic at 24 h of exposure, ~18% of cells were apoptotic by 36 h, and ~52% were apoptotic after 72 h of exposure. A similar time pattern of drug-induced apoptosis was found by DNA fragmentation assay using agarose gel electrophoresis (Fig. 1B).

Effect of As_2O_3 on Cell Cycle. As_2O_3 treatment resulted in a time-dependent accumulation of MCF-7 cells in the G_2/M phase (Fig. 2A). At time 0, only ~8% of cells were in the G_2/M phase. After 12 h of treatment, ~21% of cells were in the G_2/M phase. The value of G_2/M phase cells peaked at 24 h (~52%) and declined thereafter. Similar results were obtained with other cell lines (e.g., H460 and HeLa cells; data not shown). Microscopic examination showed that MCF-7 cells treated with 3 μM As_2O_3 for 24 h led to cell-cycle arrest at metaphase with chromosome condensation and disappearance of the nuclear envelope (Fig. 2B, b), compared with untreated cells with intact nuclei (Fig. 2B, a). These results were confirmed by DAPI staining (data not shown). For quantitative analysis of mitotic arrest, cells were stained with Wright-Giemsa, and the percentage of mitotic cells was calculated after counting at least 100 cells. As shown in Fig. 2C, ~3% of cells were at M-phase at time 0 and ~16% of cells were at M-phase at 12 h. M-phase cells reached peak value (~36%) at 24 h, and declined to ~6% after 48 h. Such a pattern for As_2O_3-induced M-phase arrest is very similar to that of the paclitaxel-induced M-phase arrest reported previously by us and others (Bhalla et al., 1993; Ling et al., 1998).

Effect of As_2O_3 on Tubulin Polymerization in Vitro. Because As_2O_3 treatment markedly blocked the cell cycle in M-phase, we became interested in testing whether As_2O_3 could directly affect tubulin. To test this hypothesis, tubulin polymerization and depolymerization in vitro were studied at room temperature in a reaction mixture containing the purified tubulin and GTP, in the presence or absence of As_2O_3. The results presented in Fig. 3A, showed that As_2O_3 significantly promoted tubulin polymerization in a concentration dependent manner. Consequently, we examined whether altered GTP binding to β-tubulin could cause As_2O_3-induced tubulin polymerization. Tubulin was preincubated with As_2O_3 at 0°C for 30 min, and then the tubulin polymerization reaction was started by the addition of GTP at room temperature. The results, as shown in Fig. 3B, indicated that pretreatment with As_2O_3 for 30 min did not affect GTP-promoted tubulin polymerization, indicating that As_2O_3-induced tubulin polymerization was not caused by interference with GTP binding domain on β-tubulin. Finally, we tested

TABLE 1

As_2O_3-induced cytotoxicity in human solid tumor cell line

Cells were treated with various concentrations of As_2O_3 at 37° C for 72 h. Cell survival was determined by 3-(4,5-dimethylthiazol-2-yl)-2,5-diphenyltetrazolium assay and IC_{50} value was calculated by graphics as described under *Materials and Methods*. Each point represents the mean ± S.D. of three independent experiments

Cell Type	Cell Line	IC_{50}	p53 Status
		μM	
Breast cancer	MCF-7	3.00 ± 0.20	WT
Cervical cancer	HeLa	4.28 ± 0.58	UK
Ovarian cancer	SK-OV-03	4.61 ± 1.10	Null
Ovarian cancer	A2780	2.80 ± 0.70	WT
Nasopharyngeal caner	KB	8.00 ± 1.00	UK
NSCLC	H661	6.40 ± 2.25	UK
NSCLC	H520	12.67 ± 2.94	MT
NSCLC	H322	13.33 ± 1.53	MT
NSCLC	H460	14.60 ± 2.50	WT

WT, wild-type; UK, unknown; MT, mutant type.

whether As_2O_3 could, like paclitaxel, stabilize tubulin polymerization. Tubulin was polymerized in the presence of GTP at room temperature for 25 min. Then the depolymerization reaction was conducted at 0°C in the presence of As_2O_3 or paclitaxel or in the absence of both drugs as control. As shown in Fig. 3C, both As_2O_3 and paclitaxel not only prevented the depolymerization of assembled tubulin but also significantly promoted the polymerization of tubulin. In contrast, the polymerized tubulin was gradually and effectively depolymerized at 0°C in the absence of both drugs. The data clearly indicate that As_2O_3 has a paclitaxel-like effect to promote and stabilize tubulin polymerization in vitro.

Effect of As_2O_3 on Cellular Microtubules. Because strong paclitaxel-like tubulin-stabilizing activity was found in vitro, we tested whether As_2O_3 treatment affected the cellular microtubule network. MCF-7 cells were treated with 0.5 μM paclitaxel, 0.1 μM vinblastine, or 3 μM As_2O_3 or with the same volume of PBS solution as control. After 12 h of incubation, the microtubule network was visualized by immunocytochemistry. The microtubule network in control cells exhibited normal arrangement and organization (Fig. 4A). Treatment with paclitaxel resulted in microtubule polymerization with an increase in the density of cellular microtubules and formation of long thick microtubule bundles surrounding the nucleus (Fig. 4B). As_2O_3 treatment resulted in findings similar to those of paclitaxel-induced microtubule changes, such as thickening and increased density of microtubules (Fig. 4C). In contrast, vinblastine treatment caused cellular microtubule depolymerization with short microtubules in the cytoplasm (Fig. 4D). To further confirm these results, we used electron microscopy to explore the effect of As_2O_3 on cellular microtubule structures in MCF-7 cells. As shown in Fig. 5, the polymerized microtubules with diameters of ~25 nm were clearly observed in ~40% of As_2O_3-treated interphase cells, whereas microtubules with such structure were seen in less than 5% of untreated control cells (Fig. 5A). Furthermore, we examined the effect of As_2O_3 on spindle formation in MCF-7 cells, and found that As_2O_3 treatment caused the formation of abnormal mitotic spindles with a circular pattern, different from paclitaxel treatment, which caused tri- or tetra-polar spindles (data not shown). All results indicated that the microtubule is the intracellular target for As_2O_3 accounting for the subsequent mitotic arrest and apoptosis.

Effect of As_2O_3 on $P34^{cdc2}$/Cyclin B Expression and Activity. It is known that the entrance to and exit from M-phase of the cell cycle is regulated by the $p34^{cdc2}$/cyclin B complex. Paclitaxel-induced M-phase arrest is associated with up-regulation and activation of $p34^{cdc2}$/cyclin B kinase in a variety of cell lines (Donaldson et al., 1994). We determined the effect of As_2O_3 on expression and activation of cdc2 and cyclin B in MCF-7 cells. As shown in Fig. 6, treatment with As_2O_3 resulted in a time-dependent up-regulation of cyclin B1, but did not change cdc2. Histone H1 kinase assay revealed that As_2O_3 treatment activated $p34^{cdc2}$/cyclin B1 kinase activity in a time-dependent manner. Similar results were obtained in H460 cells, indicating that up-regulation of cyclin B and activation of $p34^{cdc2}$/cyclin B kinase caused by As_2O_3 is not restricted to MCF-7 cells (data not shown).

Effect of As_2O_3 on Bcl-2 Phosphorylation. A number of reports have demonstrated that paclitaxel-induced M-phase arrest and apoptosis are associated with Bcl-2 phosphorylation (Blagosklonny et al., 1996; Haldar et al., 1996). We tested whether As_2O_3-induced M-phase arrest and apoptosis were associated with Bcl-2 phosphorylation. MCF-7 and H460 cells were treated with As_2O_3 for the time indicated in Fig. 7, and Bcl-2 phosphorylation was detected by immunoblotting analysis. As expected, As_2O_3 treatment resulted in a time-dependent Bcl-2 phosphorylation in both MCF-7 and H460 cells (Fig. 7). To explore whether As_2O_3-induced M-phase arrest and Bcl-2 phosphorylation could initiate apoptotic pathways, H460 cells were exposed to 10 μM As_2O_3 for 24 h. The mitotic cells (detached cells) and interphase cells (attached cells) were separated as described under *Materials and Methods*. After being washed three times with drug-free medium, the attached and detached cells were reincubated in fresh drug-free medium for the indicated time. Samples taken from the culture were divided into two parts, one for counting mitotic and apoptotic cells by Wright-Giemsa and DAPI staining, the other for determining mitotic and apopto-

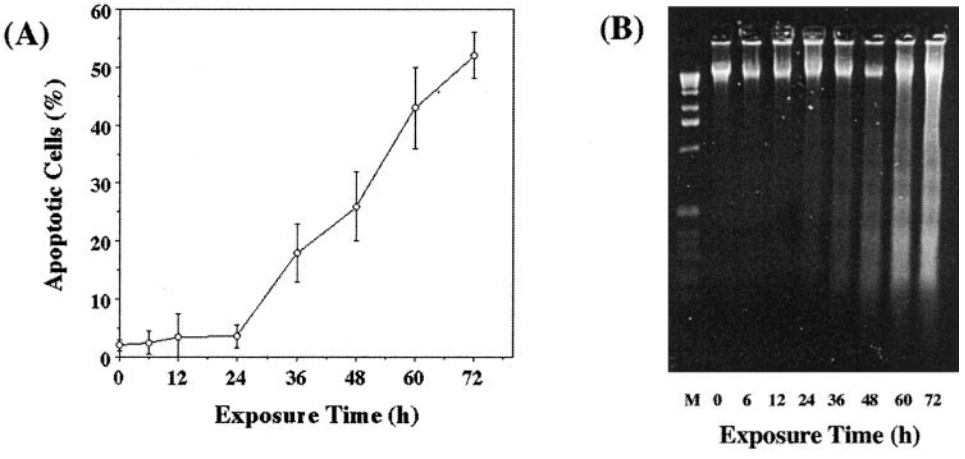

Fig. 1. As_2O_3 induces apoptosis in MCF-7 cells. A, log-phase growing cells were treated with 3 μM As_2O_3 for the indicated time points. After treatment, cells were harvested, fixed with 75% cold ethanol, and stained with 1 μg/ml of DAPI for 1 h. The apoptotic cells with nuclear breakage at least 100 cells were counted by fluorescence microscopy. Each point represents the mean ± S.D. of three independent experiments. B, As_2O_3 induces DNA laddering fragmentation. MCF-7 cells were treated with 3 μM As_2O_3 for the indicated time. After treatment, cells were lysed with lysis buffer, and DNA was extracted as described under *Materials and Methods*. DNA was dissolved in TE buffer, and subjected to electrophoresis in a 1% agarose gel. DNA laddering was visualized by UV light illumination.

tic events by immunoblotting analysis. As shown in Fig. 8, ~97% of detached cells were in M-phase at time 0. By 10 h of incubation, ~76% of cells were in M-phase; only ~4% were in M-phase at 24 h. In the detached cells, ~3% of the cells were apoptotic at time 0, which gradually increased to ~70% after 24 h of incubation. Furthermore, the immunoblotting analysis revealed that Bcl-2 phosphorylation bands in detached cells were clearly detected at time 0 but disappeared after 24 h of incubation. The cleavage bands of PARP and β-catenin were seen as early as 10 h and increased as incubation continued. In contrast, neither accumulation of mitotic or

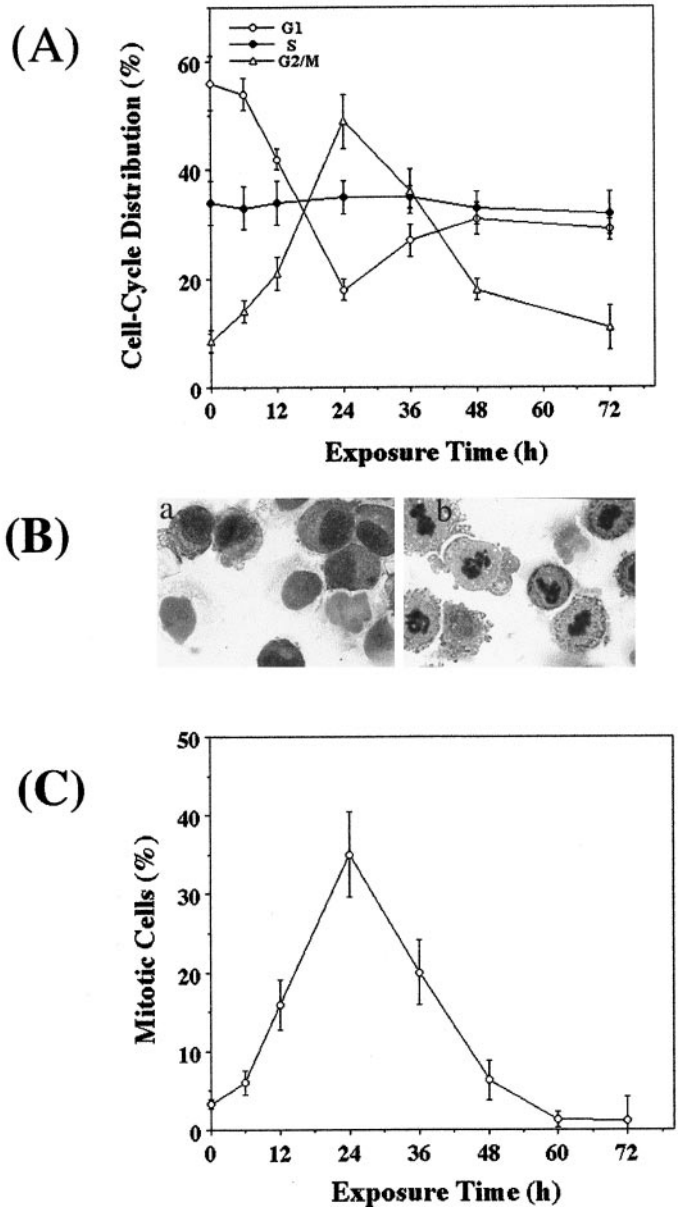

Fig. 2. Effect of As_2O_3 on cell cycle progression. A, MCF-7 cells were treated with 3 μM As_2O_3 for the indicated time points. After treatment, cells were fixed with 75% ethanol overnight, and incubated with 5 μg/ml of RNase I, and 1 μg/ml of propidium iodide for 6 h. DNA content was assessed by a flow cytometer. Each point represents the mean ± S.D. of three independent experiments. B, morphological examination of As_2O_3-induced M-phase arrest. MCF-7 cells were treated with 3 μM As_2O_3 or with the same volume of PBS solution as control. After 24 h of incubation, cells were harvested and stained with Wright-Giemsa. In As_2O_3-treated cells, typical metaphase arrest cells presented with condensed and separated chromosomes (b), whereas control cells were in interphase with intact nuclei (a). C, quantitative assessment of mitotic arrest by As_2O_3. MCF-7 cells were treated with 3 μM As_2O_3 for the indicated time. Cells were stained with Wright-Giemsa, and the mitotic cells were counted at least 100 cells. Each point represents the mean ± S.D. of three independent experiments.

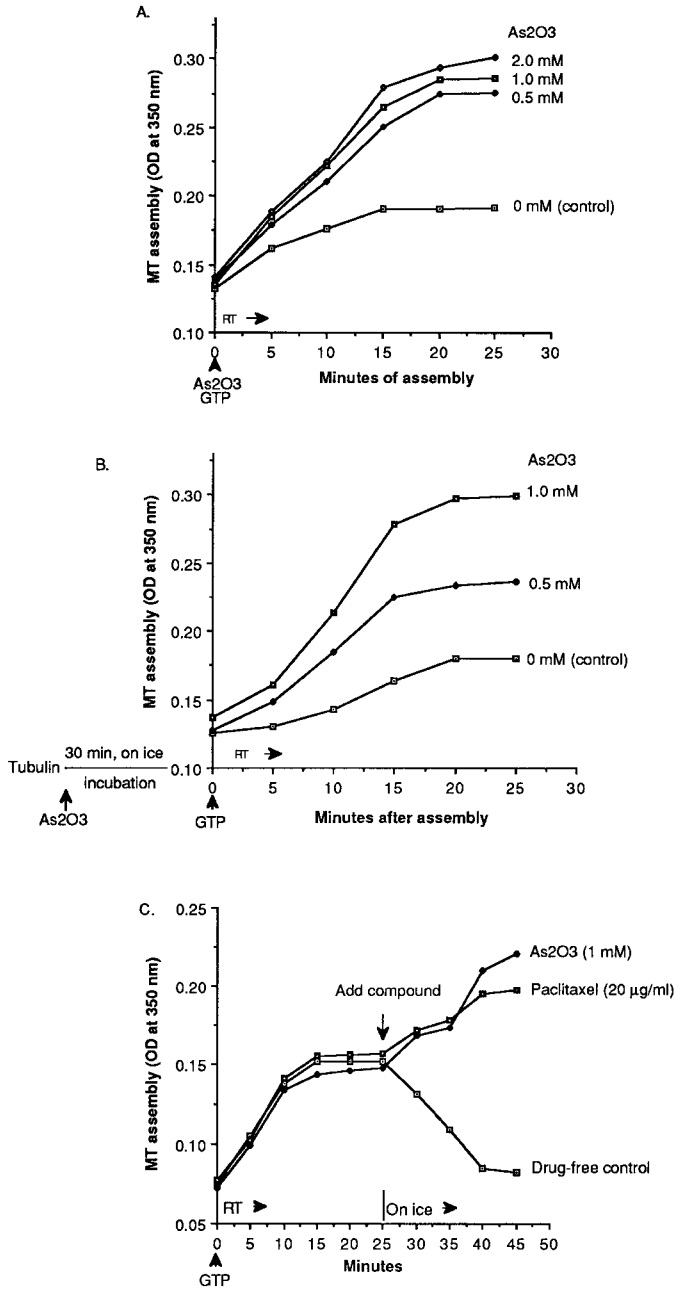

Fig. 3. Effect of As_2O_3 on microtubule polymerization in vitro. A, As_2O_3 promotes tubulin assembly. Purified bovine tubulin was incubated at 37°C in reaction mixtures containing 1 mM GTP, different concentrations of As_2O_3, and the same volume of solvent (10% NaOH) as control. Tubulin polymerization was determined by measuring observance at 350 nm. B, As_2O_3 does not affect GTP-promoted tubulin polymerization. Tubulin was pretreated with 1 mM As_2O_3 or with the same volume of solvent as control at 0°C for 30 min, then tubulin polymerization reaction was started by addition of 1 mM GTP at 37°C, and tubulin polymerization was measured as described above. C, like paclitaxel, As_2O_3 prevents against microtubule depolymerization. Tubulin was polymerized in the presence of 1 mM GTP at 37°C for 20 min. The polymerized tubulin was incubated with 1 mM As_2O_3, 10 μM paclitaxel, or with the same volume of solvent as control, and the depolymerization was performed at 0°C and monitored by measuring the absorbance value at 350 nm. Each point represents the mean value of two independent experiments. RT, room temperature.

apoptotic cells, Bcl-2 phosphorylation, cleavage of PARP, nor β-catenin was observed in attached cells. In addition, the activation of caspases (Fig. 8C) and the cleavage of procaspase-3 and -7 into the active forms (Fig. 8D) were found in detached cells as early as 10 h of incubation. The activation of caspase-3 and -7, as well as the cleavage of apoptosis-related proteins, occurred only in detached cells and as early as 10 h of incubation; by that time, ~75% of cells were still at mitosis and only ~20% were apoptotic. Thus, it is presumed that As_2O_3-induced M-phase arrest precedes initiation of apoptotic pathways and may be prerequisite.

Effect of As_2O_3 and Paclitaxel on Cell Proliferation in Drug-Resistant Cell Lines. Because As_2O_3 has paclitaxel-like activity against cell proliferation in human solid tumors, we examined whether this compound was cross resistant with paclitaxel in drug resistant cell lines. We treated parental breast cancer MCF-7 cells, P-glycoprotein–overexpressing MCF-7/Dox cells, and MRP-positive MCF-7/VP-16 cells with As_2O_3 and with paclitaxel for 72 h, and then determined the drug-induced cytotoxicities of each. As shown in Table 2, the resistance index (RI) values for paclitaxel and As_2O_3 in MCF-7/Dox cell lines were 35 and 2.3, respectively. The RI values for paclitaxel and As_2O_3 in MCF-7/VP-16 cell line were 4 and 1.9, respectively. These data indicate that As_2O_3, unlike paclitaxel, was a poor substrate for transport by both P-glycoprotein and MDR protein. Next we tested the cytotoxic effect of As_2O_3 and paclitaxel in parental ovarian cancer cell line (A2780) and its tubulin mutation paclitaxel resistant cell lines (A2780/PTx10, and A2780/PTx22). The results showed that RI values for paclitaxel were 15 and 17 in A2780/PTx10 and A2780/PTx22 cells, whereas the RI values were <1 for As_2O_3 in both tubulin mutant cell lines. These results clearly show that As_2O_3 is not cross-resistant with paclitaxel.

Discussion

Our data demonstrate that As_2O_3 is efficacious in inhibiting the proliferation of various models of human solid tumors. As_2O_3-induced cytotoxicity was independent of p53 status, suggesting that As_2O_3-induced cell death does not occur via p53-dependent pathways. We found that As_2O_3 was a poor substrate for transport by P-glycoprotein or by MRP, suggesting that pumping out intracellular As_2O_3 may not be a major factor in explaining the different susceptibilities to As_2O_3 of different cell lines. These differences remain unexplained. One possibility could be due to different cellular components and/or thresholds in different cell lines for apoptotic signaling. The IC_{50} value for As_2O_3 in MCF-7 breast carcinoma and A2780 ovarian carcinoma cell lines was about 3 μM, a concentration very close to effective serum concentration for successfully treating patients with acute promyelocytic leukemia in the clinic (Shen et al., 1997). Thus it is suggested that As_2O_3 might be useful for the treatment of some instances of human breast and ovarian cancers. In addition, we found that As_2O_3 lacked cross-resistance in both P-glycoprotein– and MRP-overexpressing cell lines. Furthermore, there is no cross-resistance between As_2O_3 and paclitaxel in two cell lines resistant to paclitaxel because of tubulin mutation, suggesting that it might be useful for treating drug-refractory patients, particularly those with paclitaxel resistance.

Although As_2O_3 has been an effective treatment for acute promyelocytic leukemia, the mechanism of action by which

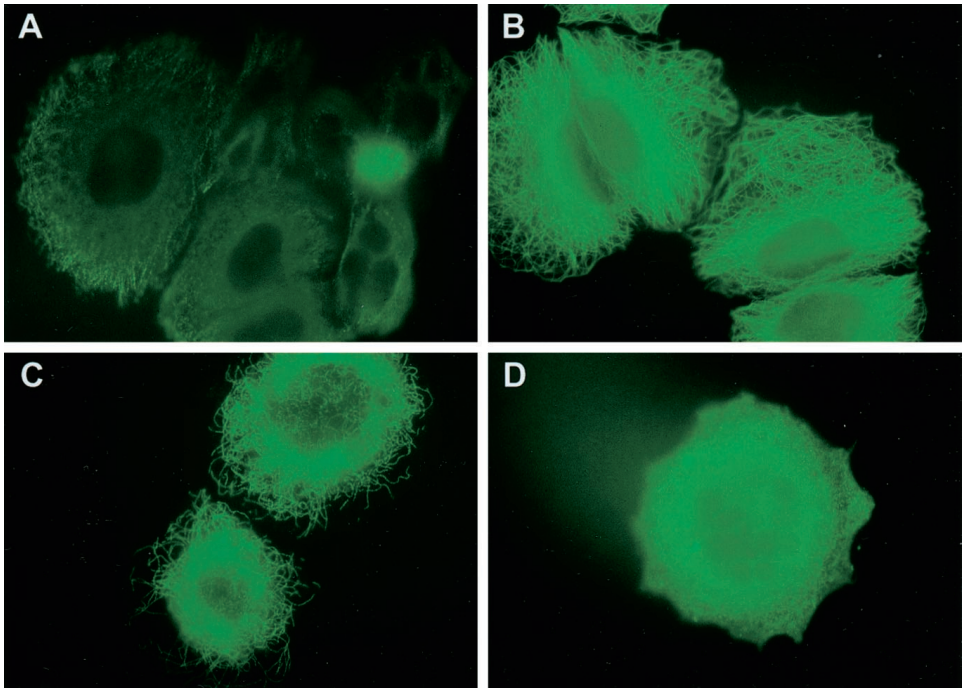

Fig. 4. Effect of As_2O_3 on the organization of cellular microtubule network. MCF-7 cells were treated with 0.5 μM paclitaxel, 0.1 μM vinblastine, and 3 μM As_2O_3, or with the same volume of PBS solution as control. After a 12-h incubation, cells were harvested and fixed with cold methanol. Cells were incubated with monoclonal anti–β-tubulin antibody at room temperature for 90 min. After incubation with FITC-conjugated second antibody, the cellular microtubules were observed by Nikon PS200 fluorescence microscopy. The normal organization of microtubule network was seen in control cells (A), the long polymerized microtubule bundles were found in both paclitaxel- and As_2O_3-treated cells (B and C), and the shortened microtubules in cytoplasm were presented in vinblastine-treated cells (D).

As_2O_3 induces cell death remains poorly understood. Recently, some investigators reported that As_2O_3 caused DNA damage, oxidative stress, and mitochondrial dysfunction (Van Wijk et al., 1988; Dong and Lou, 1993; Gurr et al., 1999; Yih and Lee, 2000). In addition, As_2O_3 treatment blocked the cell cycle in G_1 or at G_2/M depending on the cell line (Ma et al., 1998; Li and Broome, 1999). In the present study, we found that As_2O_3 treatment resulted in cell-cycle arrest at M-phase in MCF-7, H460, and HeLa cells. These results are consistent with the report by Li and Broome, who reported that As_2O_3 treatment led to metaphase arrest in myeloid leukemia cells (Li and Broome, 1999). Our results demonstrate that As_2O_3-induced M-phase arrest is due to interaction with tubulin, resulting in tubulin polymerization. We also found that tubulin polymerization by As_2O_3 did not affect GTP binding to β-tubulin. These results, however, are diametrically opposite those of Li and Broome, who reported that As_2O_3 caused blockade of GTP binding to β-tubulin and

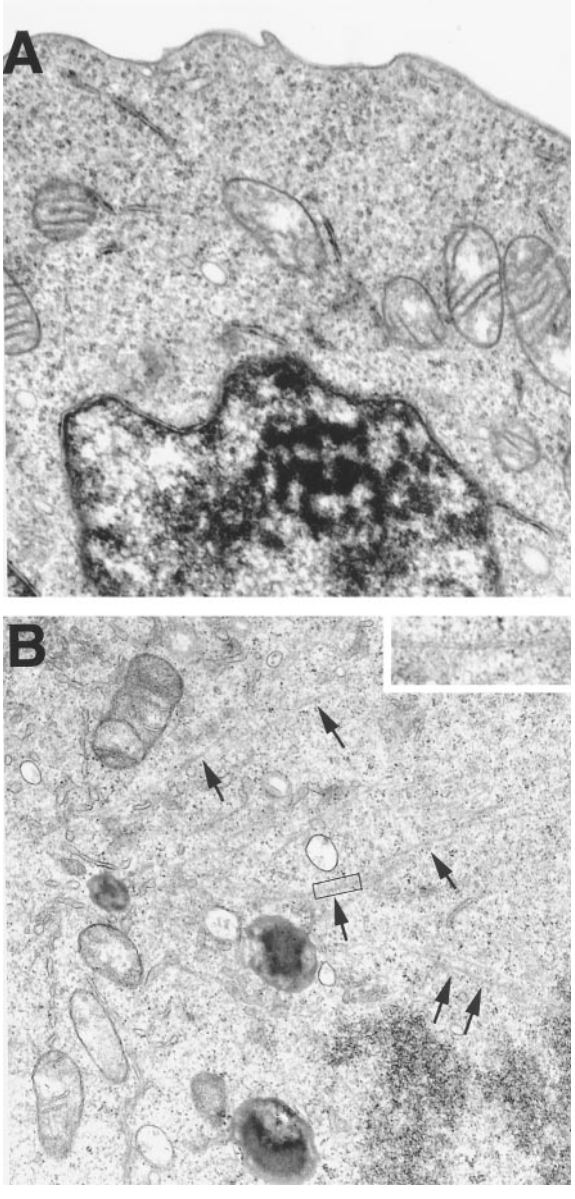

Fig. 5. As_2O_3-induced cellular microtubule polymerization seen by electron microscopy. MCF-7 cells were treated with 3 μM As_2O_3 or with the same volume of PBS solution as control. After a 12-h treatment, cells were harvested and prepared for analysis under electronic microscope as described under *Materials and Methods*. Microtubule structure is barely evident at interphase in control cells (A). The polymerized microtubule with about 25 nm tubular structure as indicated by arrow was found in As_2O_3-treated cells (B). The top in B represents the detail of polymerized microtubule structure. The magnification of the electron micrograph is 5,000×. The magnification of the insert of B on the upright is 25,000×.

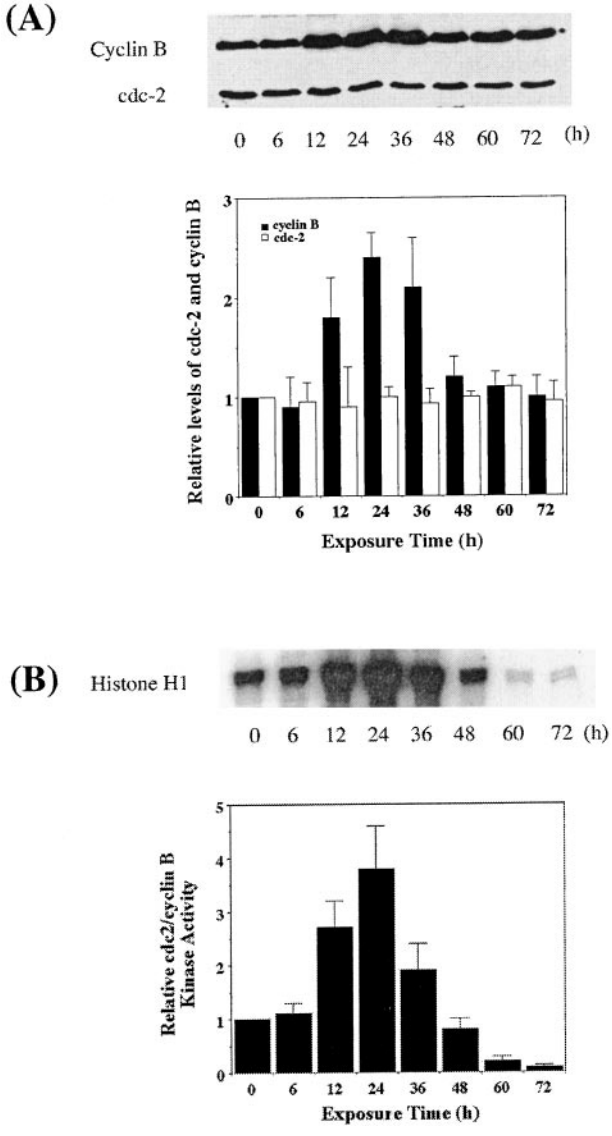

Fig. 6. As_2O_3-induced M-phase arrest is correlated with the accumulation and activation of $p34^{cdc2}$/cyclin B complex in MCF-7 cells. A, MCF-7 cells were treated with 3 μM As_2O_3 for the indicated time and then cell extracts were prepared for immunoblot analysis. Equal amounts of extract from each sample were electrophoresed on 12% SDS-PAGE. After transfer to a nitrocellulose membrane, cdc2 and cyclin B were probed by monoclonal anti-cdc2, and anti-cyclin B antibodies. The quantification of cdc2 and cyclin B was determined by laser densitometry (S-670 Scanning Densitometer; BioRad). The relative amounts of cdc2 and cyclin B were expressed as the amount compared with that at time 0. B, MCF-7cells were treated with 3 μM As_2O_3 for the indicated time. After treatment, cells were harvested and lysed with lysis buffer. Cdc2/cyclin B complexes were immunoprecipitated by monoclonal anti-cdc2 and anti-cyclin B antibodies, and protein A/G-conjugated agarose beads. Activity of cdc2/cyclin B kinase was determined by [γ-^{32}P]ATP incorporation into the substrate histone H1. The kinase activity was determined by either autoradiography, or by counting the radioactivity in histone H1 protein. The relative kinase activity was expressed as the kinase activity compared with that at time 0. Each point represents mean ± S.D. of three independent experiments

thus inhibited tubulin polymerization (Li and Broome, 1999). To certify our conclusions, we have performed the test under various conditions, including the addition of As_2O_3 before, concurrent with, and after GTP, and obtained reproducible results in all cases. Because the β-tubulin materials used by us and Li and Broome were both from Sigma-Aldrich, the explanation for contrary results is not obvious. One possibility may be the solvent for As_2O_3. In the present work, As_2O_3 was dissolved in 10% NaOH, which was also used in the drug-free control. The solvent used in Li and Broome's experiment is not clearly described, and this could be a difference.

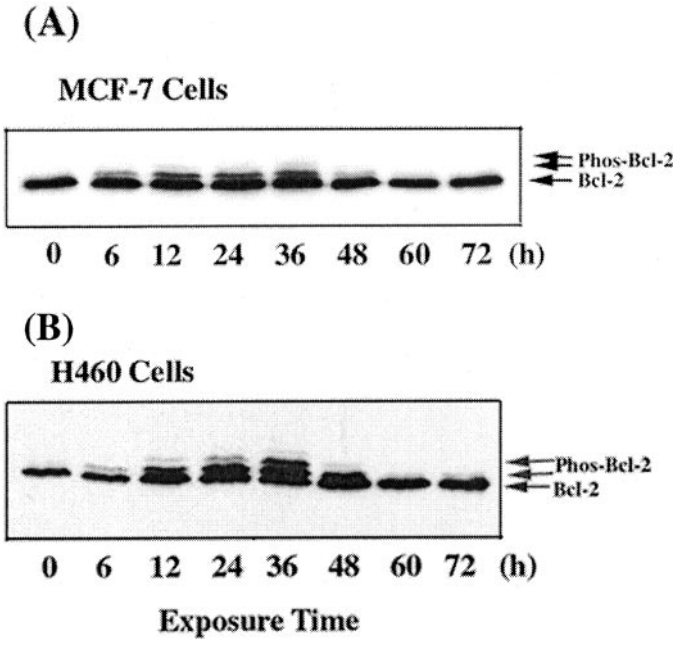

Fig. 7. As_2O_3 induces Bcl-2 phosphorylation in MCF-7 and H460 cells. MCF-7 and H460 cells were treated with 3 or 10 μM As_2O_3, respectively, for the indicated time. Cells were harvested, and cell extract was prepared and loaded on 14% SDS-PAGE as described under *Materials and Methods*. After electrophoresis, protein blots were transferred on the nitrocellulose membrane, and Bcl-2 protein was probed by monoclonal anti-Bcl-2 antibody.

In this work, we noticed a big discrepancy between the concentrations of As_2O_3 in cell-based assays and in cell-free systems. We believe that the intracellular circumstances may provide an ideal environment for the reaction of As_2O_3 with the microtubule assembly process and that the reaction conditions of the widely used cell-free microtubule assembly-disassembly assays might not facilitate the As_2O_3-microtubule interaction; consequently, the concentration of As_2O_3 in this system must be much higher than that in the cell-based assays. As a matter of fact, this phenomenon has been observed before by us using other tubulin ligands, although the discrepancies were not so pronounced (Jiang et al., 1998a,b).

Indirect immunofluorescence techniques allow detection of morphological changes in the microtubule network, such as alterations in microtubule organization and arrangement. The changes in microtubule length and density constitute an appropriate system to qualitatively assess the intracellular microtubule polymerization or depolymerization caused by antitubulin agents (de Arruda et al., 1995; Mooberry et al., 1999). The results from tubulin depolymerization experiments indicated that As_2O_3 treatment prevented tubulin depolymerization, which was similar to the effect of paclitaxel treatment. To further confirm these results, changes in the cellular microtubule network were observed immunocyto-

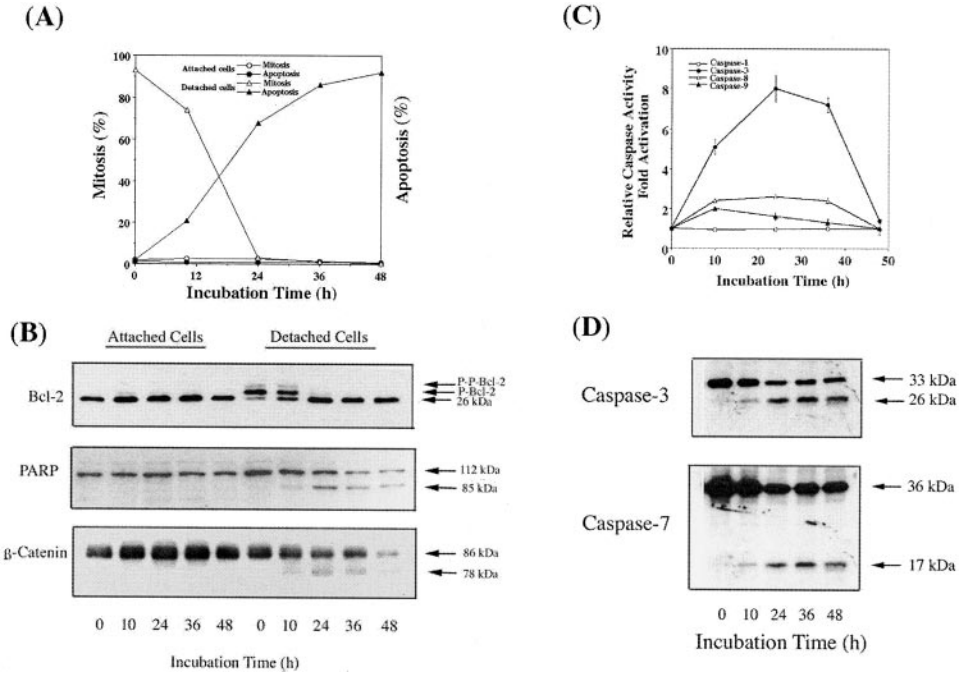

Fig. 8. As_2O_3-induced apoptotic events occurred only in mitotic cells, not in interphase cells. H460 cells were treated with 10 μM As_2O_3 for 24 h. The mitotic cells (detached) and interphase cells (attached) were separated by gentle shaking by hand. After cells were washed three times with fresh drug-free medium, they were reincubated in fresh drug-free medium with 10% serum for the indicated time. After incubation, cells were harvested and divided into two aliquots. One was for determination of M-phase arrest and apoptosis after cells stained by Wright-Giemsa and DAPI (A). The other was for determination of Bcl-2 phosphorylation, and cleavage of PARP and β-catenin (B), determination of caspase activation (C), proteolysis of procaspase-3 and procaspase-7 into activated caspase-3 and caspase-7 (D). Each point in C represents the mean ± S.D. of three independent experiments.

chemically. We found that the effect of As_2O_3 was similar to that of paclitaxel but different from that of vinblastine. Thick bundles of microtubule network surrounding the nucleus were seen in As_2O_3- and paclitaxel-treated cells, whereas shortened depolymerized microtubules were observed in vinblastine-treated cells. Details of the bundles of As_2O_3-induced microtubule were studied by electron microscopy. As_2O_3 treatment caused the formation of filament tubular structures ~25 nm in diameter. These structures were rarely seen in interphase control cells.

Antitubulin compounds can be classified into categories depending on their binding sites on β-tubulin. Vinca alkaloids, rhizoxin, dolastetins, and spongistatin react with the domain for "vinblastine"; colchicine, nocodazole, podophyllotoxin, steganacin, and curacin A bind to the "colchicine" domain (Bai et al., 1993; Uppuluri et al., 1993; Lobert et al., 1995). Paclitaxel interacts with amino acids 1 to 31 and 217 to 231 at the N terminus of β-tubulin (Rao et al., 1994, 1995); the main interaction of the paclitaxel ring with tubulin is at L279 at the B8–H9 loop (Nogales et al., 1998), and GTP/GDP adheres at the GTP binding sites (Little and Luduena, 1987). Because preincubation of β-tubulin with As_2O_3 did not prevent GTP-dependent assembly of microtubules, it suggests that the As_2O_3 binding site probably is separate from the GTP pocket. Because As_2O_3 exhibited actions on the tubulin-microtubule cycle similar to paclitaxel, As_2O_3 and paclitaxel might share a common binding domain on β-tubulin. We examined the effect of As_2O_3 on [^{3}H]paclitaxel binding to β-tubulin by competition assay as described by Bollag et al. (1995). The results from competitive inhibition experiments showed, however, that As_2O_3, even at high concentrations, did not competitively inhibit [^{3}H]paclitaxel binding to β-tubulin (data not shown), indicating that As_2O_3 does not share paclitaxel binding sites on β-tubulin. Furthermore, the results presented in Table 2 show that there is no cross-resistance between As_2O_3 and paclitaxel in paclitaxel-resistant cell lines due to tubulin mutation, further supporting the interpretation that As_2O_3 has its own binding site on β-tubulin.

In eukaryotic cells, cell-cycle progression is regulated although timely activation and inactivation of cyclin-dependent kinases, cyclins, and other regulatory factors. Inappropriate alteration in the expression or/and activation of cyclin-dependent kinases and regulators can lead to blockade of cell cycle progression and induction of programmed cell death (Pines, 1995). It is well known that $p34^{cdc2}$/cyclin B complexes are involved in regulation of G_2/M phase and the M-phase transition (King et al., 1994). Our previous work and that of others have demonstrated that paclitaxel-induced M-phase arrest, inappropriate accumulation of B type cyclins and activation of $p34^{cdc2}$/cyclin B kinase was associated with the initiation of apoptotic pathways. In the present study, we found that As_2O_3 treatment led to an increase in cyclin B level and stimulation of $p34^{cdc2}$/cyclin B kinase activity. The pattern of As_2O_3-induced activation of $p34^{cdc2}$/cyclin B and apoptosis is similar to that of paclitaxel, as we described previously (Ling et al., 1998a). Our results indicate that in addition to direct disruption of tubulin, treatment with As_2O_3 can lead to inappropriate accumulation and/or activation of G_2/M phase-related regulators, resulting in the initiation of apoptosis signaling.

Recently, a number of investigators indicated that antitubulin agents are able to induce Bcl-2 phosphorylation (Jiang et al., 1998a; Tahir et al., 2001). The role of Bcl-2 phosphorylation in G_2/M phase arrest and in apoptosis remains to be further elucidated (Yamamoto et al., 1999). Our previous results indicated that some anti-tubulin agents, such as nocodazole, induced Bcl-2 phosphorylation that correlated only with M-phase arrest. Paclitaxel-induced Bcl-2 phosphorylation was associated with the initiation of apoptosis, however (Ling et al., 1998b). As_2O_3 treatment, like that of most antitubulin agents, resulted in Bcl-2 phosphorylation in MCF-7 and H460 cells. As_2O_3-induced apoptotic events including the activation of caspases and proteolysis of apoptotic target proteins occurred only in drug-induced mitotic cells, not in interphase cells. A time-course study showed that As_2O_3-induced Bcl-2 phosphorylation preceded by 10 h the activation of caspase-3 and -7 and cleavage of PARP and β-catenin, suggesting that As_2O_3-induced M-phase arrest and Bcl-2 phosphorylation might be a required event for the initiation of apoptosis. Recent reports indicate that antitubulin agent blockage of the cell cycle at M-phase can be associated with the activation of several types of kinases, leading to the phosphorylation of cascades, and the activation of cdc2/cyclin B kinase, cdc-25, Raf, and Bcl-2 phosphorylation (Scatena et al., 1998; Fang et al., 2000). To explore the kinases that might be involved in As_2O_3-induced Bcl-2 phosphorylation, we used pharmacological concentrations of kinase inhibitors to test their effect on drug-induced M-phase arrest and Bcl-2 phosphorylation. Preliminary data show that the protein kinase C inhibitor staurosporine at 50 nM effectively prevented As_2O_3-induced Bcl-2 phosphorylation and M-phase arrest; the cdc2 kinase inhibitor roscovitine partially inhibited Bcl-2 phosphorylation. However, the tyrosine kinase inhibitor genistein and the mitogen-activated protein kinase inhibitor PD98059 had no effect on Bcl-2 phosphorylation (unpublished data). These data suggest that the activation of some specific kinases, such as protein kinase C, could be responsible for As_2O_3-induced Bcl-2 phosphorylation and M-phase arrest.

In summary, our data demonstrate that As_2O_3 is efficacious in suppressing the cell growth in a variety of solid tumor models. As_2O_3 directly interferes with microtubules, blocking cell cycle at the M-phase. These effects are paclitax-

TABLE 2

As_2O_3-induced cytotoxicity in drug-sensitive and -resistant cell lines

Cells were treated with different concentration of drugs at 37° C for 72 h. Cell survival was determined by 3-(4,5-dimethylthiazol-2-yl)-2,5-diphenyltetrazolium assay, and IC_{50} was calculated as described under *Materials and Methods*. Each value represents the mean ± S.D. of three independent experiments. Resistance index = IC_{50} in resistant cells/IC_{50} in parental cells.

Cell Lines	IC_{50}	
	As_2O_3	Paclitaxel
	μM	
MCF-7	3.00 ± 0.20	0.66 ± 0.33
MCF-7/Dox (P-gp positive)	7.00 ± 1.70	23.30 ± 10.69
Resistance index	2.3	35
MCF-7/VP-16 (MRP positive)	5.56 ± 2.11	2.57 ± 1.36
Resistance index	1.9	4
A2780	2.80 ± 0.70	0.04 ± 0.08
A2780/PTX10 (tubulin mutant)	2.41 ± 0.92	0.59 ± 0.16
Resistance index	0.86	15
A2780/PTX22 (tubulin mutant)	2.61 ± 1.36	0.66 ± 0.13
Resistance index	0.93	17

P-gp, P-glycoprotein.

el-like, but totally distinct from paclitaxel: As_2O_3 is more active than paclitaxel in MDR and MRP cell lines and equally active in cell lines in which mutation in the tubulin binding site for paclitaxel renders that drug 15-fold less potent. Similar to most antitubulin agents, As_2O_3 causes inappropriate accumulation and activation of $p34^{cdc2}$/cyclin B, Bcl-2 phosphorylation, and, finally, triggering of the apoptotic cascade. Such a unique mechanism for As_2O_3 indicates that it may be useful for treating patients with solid tumors either alone or in combination with other therapeutic agents.

References

Bai R, Cherry ZA, Herald CL, Pettit GR, and Hamel E (1993) Spongistatin1, a highly cytotoxic, sponge-derived, marine natural product that inhibits mitosis, microtubule assembly and the binding of vinblastine to tubulin. *Mol Pharmacol* **44:**757–766.

Bhalla K, Ibrado AM, Tourkina CQ, Tang CQ, Mahoney ME, and Huang Y (1993) Taxol induces internucleosomal DNA fragmentation associated with programmed cell death in human myeloid leukemia. *Leukemia* **7:**563–568.

Blagosklonny MV, Schulte T, Nguyen P, Trepel J, and Neckers LM (1996) Taxol-induced apoptosis and phosphorylation of Bcl-2 protein involves c-Raf-1 and represents a novel c-Raf-1 signal transduction pathway. *Cancer Res* **56:**1851–1854.

Bollag DM, McQueney PA, Zhu J, Hensens O, Koupal L, Liesch J, Goetz M, Lazarides E, and Woods CM (1995) Epothilones, a new class of microtubule-stabilizing agents with a Taxol-like mechanism of action. *Cancer Res* **55:**2325–2333.

Chen GQ, Shi XG, Tang W, Xiong SM, Zhu J, Cai X, Han ZG, Ni JH, Shi GY, Jia PM, et al. (1997) Use of arsenic trioxide (As_2O_3) in the treatment of acute promyelocytic leukemia (APL): I. As_2O_3 exerts does-dependent dual effects on APL cells. *Blood* **89:**3345–3353.

Chen GQ, Zhu J, Shi XG, Ni JH, Zhon HJ, Si GY, Jin XL, Tang W, Li XS, Xiong SM, et al. (1996) In vitro studies on cellular and molecular mechanisms of arsenic trioxide (As_2O_3) in the treatment of acute promyelocytic leukemia: As_2O_3 induces NB4 cells apoptosis with downregulation of Bcl-2 expression and modulation of PML-RARα/PML proteins: *Blood* **88:**1052–1061,.

Chen YC, Lin-Shiau SY, and Lin JK (1998) Involvement of reactive oxygen species and caspase 3 activation in arsenite-induced apoptosis. *J Cell Physiol* **177:**324–333.

de Arruda M, Cocchiaro CA, Nelson CM, Grinnell CM, Janssen B, Haupt A, and Burlozzari T (1995) LU103793 (NSC D-669356): a synthetic peptide that interacts with microtubules and inhibits mitosis. *Cancer Res* **55:**3085–3029.

Donaldson KL, Goolsby G, Kiener PA, and Wahl AF (1994) Activation of $p34^{cdc2}$ coincident with Taxol-induced apoptosis. *Cell Growth Differ* **5:**1041–1050.

Dong JT and Lou XM (1993) Arsenic-induced DNA-strand breaks associated with DNA-protein crosslinks in human fetal lung fibroblasts. *Mutat Res* **302:**97–102.

Fang M, Du L, Stone AA, Gilbert KM, and Chambers TC (2000) Modulation of mitogen-activated protein kinases and phosphorylation of Bcl-2 by vinblastine represent persistent forms of normal fluctuations at G2-M. *Cancer Res* **60:**6403–6407.

Giannakakou P, Sackett DL, Kang YK, Zhang Z, Buters JT, Fojo T, and Poruchynsky MS (1997) Paclitaxel-resistant human ovarian cancer cells have mutant β-tubulins that exhibit impaired paclitaxel-driven polymerization. *J Biol Chem* **272:**17118–17125.

Gurr J-R, Bau D-T, Liu F, Lynn S, and Jan K-Y (1999) Dithiothreitol enhances arsenic trioxide-induced apoptosis in NB4 cells. *Mol Pharmacol* **56:**102–109.

Haldar S, Chintapalli J, and Croce CM (1996) Taxol induces bcl-2 phosphorylation and death of prostate cancer. *Cancer Res* **56:**1253–1255.

Hansen MB, Nielson SE, and Berg K (1989) Re-examination and further development of a precise and rapid dye method for measuring cell growth/cell kill. *J Immunol Methods* **119:**203–210.

Hei TK, Liu SX, and Waldren C (1998) Mutagenicity of arsenic in mammalian cells: Role of reactive oxygen species. *Proc Natl Acad Sci* **95:**8103–8107.

Hyams JF and Lloyd CW (1993) *Microtubules*. Wiley-Liss, New York

Jiang JD, Davis AS, Middleton K, Ling YH, Perez-Soler R, Holland JF and Bekesi G (1998a) 3-(Iodoacetamido)-benzoylurea: a novel cancericidal tubulin ligand that inhibits microtubule polymerization, phosphorylates bcl-2 and induces apoptosis in tumor cells. *Cancer Res* **58:**5389–5395.

Jiang JD, Wang Y, Roboz J, Strauchen J, Hooland JF, and Bekesi JG (1998b) Inhibition of Microtubule Assembly in tumor cells by 3-bromoacetylamino benzoylurea, a new cancericidal compound. *Cancer Res* **58:**2126–2133.

Jordan MA, Thrower D, and Wilson L (1992) Effects of vinblastine, podophyllotoxin and nocodazole on mitotic spindles: implications for the role of microtubule dynamics in mitosis. *J Cell Sci* **102:**401–416.

King RW, Jackson PK, and Kirschner MW (1994) Mitosis in transition. *Cell* **79:**563–571.

Kroemer G and de The H (1999) Arsenic trioxide, a novel mitochondriotoxic anticancer agents? *J Natl Cancer Inst* **91:**743–745.

Li YM and Broome J (1999) Arsenic targets tubulins to induce apoptosis in myeloid leukemia cells. *Cancer Res* **59:**776–780.

Ling YH, Consoli U, Tornos C, Andreeff M, and Perez-Soler R (1998a) Accumulation of cyclin B1, activation of cyclin B1-dependent kinase and induction of programmed cell death in human epidermoid carcinoma KB cells treated with taxol. *Int J Cancer* **75:**925–932.

Ling YH, El-Naggar AK, Priebe W, and Perez-Soler R (1996) Cell cycle-dependent cytotoxicity, G2/M phase arrest and disruption of $p34^{cdc2}$/cyclin B1 activity induced by doxorubicin in synchronized P388 Cells. *Mol Pharmacol* **49:**832–841.

Ling YH, Tornos C, and Perez-Soler R (1998b) Phosphorylation of bcl-2 is a marker of M-phase events and not a determinant of apoptosis. *J Biol Chem* **273:**18984–18991.

Little M and Luduena RF (1987) Location of two cysteines in brain β1-tubulin that can be cross-linked after removal of exchangeable GTP. *Biochim Biophys Acta* **912:**28–33.

Lobert S, Frankfurter A, and Correia JJ (1995) Binding of vinblastine to phosphocellulose-purified and $\alpha\beta$-class III: the role of nucleotides and β-tubulin isotypes. *Biochemistry* **34:**8050–8060.

Look AT (1998) Arsenic and apoptosis in the treatment of acute promyelicytic leukemia. *J Natl Cancer Inst* **90:**86–88.

Ma DC, Sun YH, Chang KZ, Ma XF, Huang SL, Bai YH, Kang J, Liu YG, and Chu JJ (1998) Selective induction of apoptosis of NB4 cells from G2+M phase by sodium arsenite at low doses. *Eur J Haematol* **61:**27–35.

Margolis RL and Wilson L (1998) Microtubule treadmilling: what goes around comes around. *Bioessays* **20:**830–836.

Meada H, Hori S, Nishitoh H, Ichijo H, Ogawa O, Kakchehi Y, and Kkizuka A (2001) Tumor growth inhibition by arsenic trioxide (As_2O_3) in the orthotopic metastasis model of androgen-independent prostate cancer. *Cancer Res* **61:**5432–5440.

Mitchison TJ (1988) Microtubule dynamics and kinetochores function in mitosis. *Annu Rev Cell Biol* **4:**527–549.

Mooberry SL, Tien G, Hernandez AH, Plubrukarn A, and Davidson BS (1999) Laulimalide and isolaulimalide, new paclitaxel-like microtubule-stabilizing agents. *Cancer Res* **59:**653–660.

Nogales E, Wolf SG, and Downing KH (1998) Structure of the $\alpha\beta$ tubulin dimmer by electron crystallography. *Nature (Lond)* **391:**199–202.

Perez-Soler R, Neamati N, Zou YY, Schneider E, Doyle LA, Andreeff M, Priebe W and Ling YH (1997) Annamycin circumvents resistance mediated by the multidrug resistance-associated protein (MRP) in breast MCF-7 and small-cell lung UMCC-1 cancer cell lines selected for resistance to etoposide. *Int J Cancer* **71:**35–41.

Perkins C, Kim CN, Fang G, and Bhalla K (2000) Arsenic induces apoptosis of multidrug-resistant human myeloid leukemia cells that express Bcr-Abl or overexpress MDR, MCP Bcl-2 or Bcl-XL. *Blood* **95:**1014–1022.

Pines J (1995) Cyclins, CDKs and cancer. *Semin Cancer Biol* **6:**63–72.

Rao S, Krauss NE, Heerding JM, Swindell CS, Ringel I, Orr GA, and Horwitz SB (1994) 3′-(*p*-azidobenzamido) taxol photolabel the N-terminal 31 amino acids of β-tubulin. *J Biol Chem* **269:**3132–3134.

Rao S, Orr GA, Chaudhary AG, Kingstone DGI, and Horwitz SB (1995) Characterization of the Taxol binding site on the microtubule. *J Biol Chem* **270:**20235–20238.

Rowinsky EK and Donehower RC (1991) The clinical pharmacology and use of antimicrotubule agents in cancer chemotherapeutics. *Pharmacol Ther* **52:**35–84.

Scatena CD, Stewart ZA, Mays D, Tang LJ, Keefer CJ, Leach SD, and Pietenpol JA (1998) Mitotic phosphorylation of Bcl-2 during normal cell cycle progression and Taxol-induced growth arrest. *J Biol Chem* **273:**30777–30784.

Seol JG, Park WH, Kim ES, Jung CW, Hyun JM, Kim BK, and Lee YY (1999) Effect of arsenic trioxide on cell cycle arrest in head and neck cancer line PCl-1. *Biochem Biophys Res Commun* **265:**400–404.

Shao W, Fanelli M, Ferrara FF, Riccioni R, Rosenauer A, Davison K, Lamph WW, Waxman S, Pelicci PG, Lo Coco F, et al. (1998) Arsenic trioxide as an inducer of apoptosis and loss of PML/RARα protein in acute promyelocytic leukemia cells. *J Natl Cancer Inst* **90:**124–1133.

Shen ZX, Chen GQ, Ni JH, Lin XS, Xiong SM, Qiu QY, Zhu J, Tang W, Sun GL, Yang KQ, et al. (1997) Use of arsenic trioxide (As_2O_3) in the treatment of acute promyelocytic leukemia (APL): II. Clinical efficacy and pharmacokinetics in relapsed patients. *Blood* **89:**3354–3360.

Soignet SL, Maslak P, Wang ZG, Jhanwar S, Calleja E, Dardashti LJ, Corso D, DeBlasio A, Gabrilove J, Scheinberg DA, et al. (1998) Complete remission after treatment of acute promyelocytic leukemia with arsenic trioxide. *N Engl J Med* **339:**1341–1348.

Tahir SK, Han EK, Credo B, Jae H-S, Pietenpol JA, Scatena CD, Wu-Wong JR, Frost D, Sham H, Rosenberg SH, et al. (2001) A-204197, a new tubulin-binding agent with antimitotic activity in tumor cell lines resistant to known microtubule inhibitors. *Cancer Res* **61:**5480–5485.

Uppuluri S, Knipling L, Sackett DL, and Wolff J (1993) Localization of the colchicine-binding site of tubulin. *Proc Natl Acad Sci USA* **90:**11598–11620.

Van Wijk R, Welters M, Souren JE, Ovelgonne H, and Wiegant FA (1988) Serum-stimulated cell cycle progression and stress protein synthesis in C3H10T1/2 fibroblasts treated with sodium arsenite. *Oncogene* **3:**163–168.

Yamamoto K, Ichijo H, and Korsmeyer SJ (1999) Bcl-2 phosphorylation and inactivated by an ASK1/Jun N-Terminal protein kinase pathway normally activated at G2/M. *Mol Cell Biol* **19:**8469–8478.

Yih L-H and Lee T-C (2000) Arsenite induces p53 accumulation through an ATM-dependent pathway in human fibroblasts. *Cancer Res* **60:**6346–6352.

Zhu XH, Shen YL, Jing Y, Cai X, Jia PM, Huang Y, Tang W, Shi GY, Sun Y, Dai J, Wang ZY, and Chen SJ (1999) Apoptosis and growth inhibition in malignant lymphocytes after treatment with arsenic trioxide at clinically achievable concentrations. *J Natl Cancer Inst* **91:**772–778.

Address correspondence to: Dr. Yi-He Ling, Comprehenisve Cancer Center, Albert Einstein College of Medicine, Jack and Pearl Resnick Campus, 1500 Morris Park Avenue, Bronx, New York, 10461. E-mail: yling@aecom.yu.edu